M. DUNĐER, Ž. IVANDIĆ, I. SAMARDŽIĆ

ISSN 0543-5846
METABK 47(4) 325-330 (2008)
UDC – UDK 621.791.052 669.15 : 519.28. 539.63=111

SELECTION OF ARC WELDING PARAMETERS OF MICRO ALLOYED HSLA STEEL

Received – Prispjelo: 2007-05-28
Accepted – Prihvaćeno: 2008-02-13
Original Scientific Paper – Izvorni znanstveni rad

In order to ensure performance reliability of a welded product, its quality has to be ensured by proper setting of welding parameters and welding cycle. A quality weld – a weld with no manufacturing, structural or geometric flaws, i.e. with necessary mechanical properties - is achieved only by correct parameter definition and adherence. The knowledge of various effects and relations between welding parameters and their repetition enable an optimal choice of welding parameters.

Key words: HSLA, Welding parameters, Cooling time Δt8/5, Hardness, Impact energy

Izbor parametara elektrolučnog zavarivanja mikrolegiranog HSLA čelika. Za pouzdan rad zavarenog proizvoda potrebno je kvalitetu osigurati pravilnim određivanjem parametara i slijeda zavarivanja. Pravilnim propisivanjem i provođenjem parametara zavarivanja osigurava se kvalitetan zavar, zavar bez proizvodnih, strukturnih i geometrijskih grešaka, odnosno s potrebnim mehaničkim svojstvima. Poznavanje utjecaja i odnosa između parametara zavarivanja te njihova ponovljivost omogućuje izbor i propisivanje optimalnih parametara zavarivanja.

Ključne riječi: Mikrolegirani čelici povišene čvrstoće, parametri zavarivanja, vrijeme hlađenja $\Delta t_{8/5}$ tvrdoća, udarna radnja loma

INTRODUCTION

Like all steel types, HSLA requires a definition and strict practical adherence to welding parameters in order to achieve the required weld quality.

Different sources offer a varying array of welding parameters. Although their hierarchical importance can be disputed, their principal definition and practical adherence are prerequisites for the quality of welded joints [1,2].

The analysis of earlier data from tests on steels of same or similar mechanical properties and chemical compositions enable pinpoint testing of new steels, shorter and cheaper research and a comparison of results obtained by different authors.

A contribution to weldability research of this particular group of steels will increase the reliability of welded joints – this is of particular importance for products at higher risk of manufacturing flaws, as well as Stress Corrosion Cracking (SCC) and failure during exploitation.

DEFINITION OF THE RESEARCH PROBLEM

Reliability and quality requirements are being set in order to prevent possible flaw-originating failures of welded joints under exploitation. It could be said that the exact determination of welding parameters and cycle orders is the precondition for failsafe product performance. Due to a wide range of welding consumables, technologies, parameters and final properties, design engineers, technologists and manufacturers are dependant on each other when selecting the most feasible and economic combination of consumable, welding technology and welding parameters, thus satisfactory properties of a welded construction as a whole. Beside altering the quality of joints by varying welding parameters, energy consumption and consequently welding costs are being also affected. Ideally, required weld properties and weld reliability should be paired with minimal welding costs (i.e. material and energy). The main variables in a welding process are: welding current, welding arch voltage, welding speed, i.e. cooling time from 800°C to 500°C ($\Delta t_{8/5}$) and spefic heat input.

The selection of primary and secondary energy is the basis for any welding technology. Pre-heating energy input and heat penetrating into the base material during a welding cycle are characterised by specific thermal properties which cause the formation of a thermic field. The thermic field directly affects mechanical characteristics of the material structure, particularly in the Heat Affected Zone (HAZ).

In order to understand better the variety of difficulties related to HSLA pressure vessels, one should consider research results of the influence of thermic fields on microstructure transformations during welding, which is

M. Dunđer, Holdina d.o.o. Bosnia and Herzegovina. Ž. Ivandić, I. Samardžić, Faculty of Mechanical Engineering University of Osijek, Slavonski Brod, Croatia.

Table 1 **Chemical composition and mechanical properties of HSLA TStE 420**

Steel	Chemical composition / mass %;									
	C	*Si*	*Mn*	*P*	*S*	*Ni*	*N*	*Al*	*V*	*Cu*
TStE 420	0,18	0,3	1,47	0,017	0,005	0,22	0,016	0,023	0,13	0,02
	Mechanical properties at standard room temperature									
	Yield Strength $R_{p0,2}$ / MPa		Tensile Strength R_m / MPa		Elongation A_5 / %		Contraction Z / %		Bending α=180 °	
									Longit.	Trans.
	422	577	30	61,9					+	+
	Impact energy, K_V / J at 20°C, 0°C, -20°C and -40°C, longitudinally									
	40J, 27J and 20J according to data [5], testing results: 261J, 245J and 182J									

affecting mechanical properties of the welded joint. [3] This particular influence can be expressed with reference to cooling speed, i.e. the duration of cooling from 800°C to 500°C ($\Delta t_{8/5}$) during structure transformation [4].

For that very purpose, FSB in Zagreb (The Faculty of Mechanical and Naval Engineering) and Strojniška fakulteta in Maribor (The Mechanical Engineering Faculty) have conducted an excessive research. This paper offers test results for cooling speed effect in significant relation to hardness and tensile strength of HSLA TStE 420.

The Choice of Base Material

HSLA TStE 420 was selected for experimental research because pressure vessels – rail wagons for the transportation and storage of liquefied oil gas – have been produced recently by using that material. These steels have not been sufficiently researched yet, but current experience with the use of micro-alloyed steel suggests certain risks of Stress Corrosion Cracking (SCC) on pressure vessels in the current use.

Table 1 shows the chemical composition and mechanical properties of the examined steel.

Hardness Testing of Real Welded Joints

Oftentimes, hardness data for a given welded joint are not presented as complete information, which could be used by the welding expert for further weldability analysis and exploitation behaviour with sufficient reliability. The hardness of the welded joint and of the base material can be observed from an angle of statistic sample theory – the final measurement result can represent any value within a basic hardness group. Result dissipation is larger with welded joints than with the base material because the welded joint consists of weld material and HAZ, which both again have different zones.

The hardness of a welded joint is usually measured in line with recommendations entailed in the IIW document IX-1609-90 [6], by using a contour method and measurement across the welded joint. Figure 1 illustrates cross-section hardness measurement on a real welding sample.

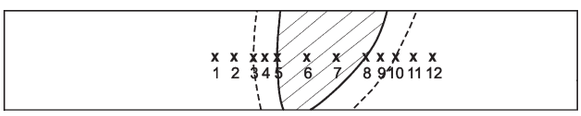

Figure 1. Cross-section hardness measurement on a real welding sample

Testing of Impact Energy by Using the Charpy-V Method

Decreasing tensile strength in HAZ is usually the consequence of "transformational hardening". Primarily, this phenomenon occurs due to $\alpha \rightarrow \gamma \rightarrow \alpha$ microstructural transformations. The exact nature of these transformations depends on chemical properties of the particular steel and on maximal temperature and cooling speed - that being expressed as cooling time between 800°C to 500°C ($\Delta t_{8/5}$). The expected microstructures can be predicted by using available diagrams for selected steels, or can be calculated based on defined relations in some cases. Increased grain growth indicates brittle behaviour of the particular zone.

The dent location is of crucial importance for tensile strength testing of HAZ, causing wide result scattering and thus low reliability of the analysis.

To avoid this phenomenon in the described analysis, each specimen of real welds was frontally etched and the test specimen was produced after denting.

The weld position was perpendicular to the direction of base material rolling. A nearly equal penetration of single layers was achieved on the vertical side.

Welded plates were thermally isolated in order to achieve desired cooling speed and to avoid thermal losses

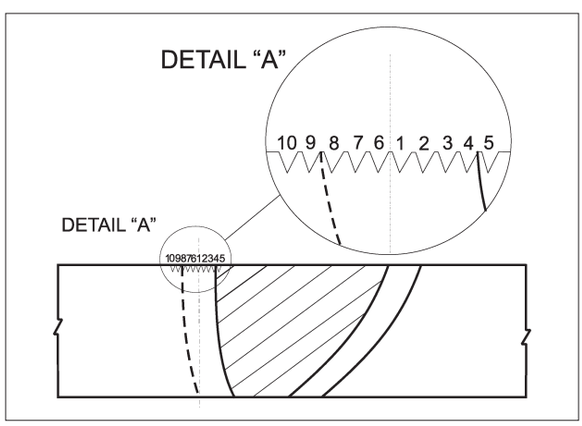

Figure 2. Experimental determination of the dent tip of minimal impact energy

through physical supports. The plates were not clammed.

In order to determine the particular HAZ of minimal impact energy, specific impact energy values were established across HAZ. Specimens had a "V"-notch of varying distance to the melting line.

Notch tip position was altered by 0,5mm to the left and to the right relative to the line indicating the notch tip in Figure 2. Ten specimens were tested for each cooling time ($\Delta t_{8/5}$= 5, 10, 25 and 50s) at temperature of 20°C, five times to each side of the line.

Once the minimal impact energy was established, further tests were run to establish the critical weld area and HAZ. That strain shows impact energy behaviour of the most critical weld area at given welding parameters. For preset welding parameters, it entails data needed to determine the particular temperature for minimal impact energy in the critical weld area under unfavourable conditions.

RESEARCH RESULTS

Hardness testing and minimal impact energy testing for real welded joints of HSLA TStE 420 were foreseen by the experiment plan. Base material thickness was 15 mm.

During real cycle welding tests, welding for the cooling time $\Delta t_{8/5}$= 5s was set up as indicated in Figure 3. Welding for $\Delta t_{8/5}$ = 10, 25 and 50s and a ½ "V" notch in a 15 mm plate was set up as shown in Figure 4.

Cooling time $\Delta t_{8/5}$ as measured by using Ni-CrNi thermocouple sunk into the melt is illustrated in Figure 5.

Because it is impossible to obtain cooling time $\Delta t_{8/5}$ = 5s in a set-up as shown in Figure 4, a set-up as illustrated in Figure 3 was used. Cooling strains were recorded by computer; "Matex" application was used. As planned for the experiment, MAG technology was chosen and average values of set welding parameters were recorded on-line. In addition, welding parameters were also recorded digitally. For both recording methods, received data was found to match fully (with no discrepancy). Welding parameters (voltage, welding current, welding speed), wire diameter and heat input for each weld are given in Table 2.

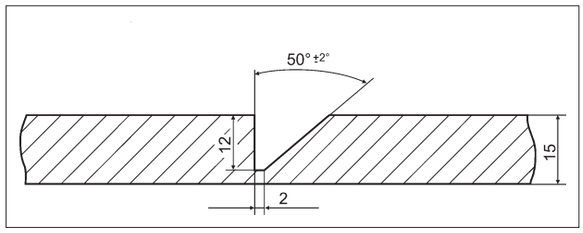

Figure 3. Illustration of the set-up for real sample welding at cooling time $\Delta t_{8/5}$= 5s

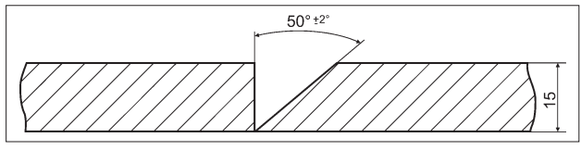

Figure 4. Illustration of the set-up for real sample welding at cooling time $\Delta t_{8/5}$= 10, 25 and 50 s

Figure 5. Sinking of Ni-Cr Ni thermocouple into the melt

Table 2 **MIG welding parameters for characteristic samples**

Plate No.	Plate 1	Plate 2	Plate 3	Plate 4
Wire Ø(mm)	1,6	1,6	1,6	1,6
T_0 (°C)	17	17	17	17
v (cm/min)	40,0	35,4	31,0	24,2
$\Delta t_{8/5}$ (s)	5,0	10,0	25,0	50,0
I (A)	220	220	225	230
U (V)	24	24	24	24,5
E (J/mm)	1332	1491	2250	2328

(Oscillatory) one-pass welding was used except for plate No. 1 where no oscillation was applied. Oscillation amplitude was 10 mm at a rate of 35 oscillations per minute. The inert gas used was CO_2 at a flow rate of 15 l/min. For all recordings, wire feed speed was 6 m/min; the distance between the contact tube and base metal was 18 mm. Flux-cored wire FILTUB 12B ø1,6 mm, produced by "Elektroda Jesenice" was used during one-pass welding. The chemical composition and mechanical properties of pure weld metal are given in Table 3, as indicated in the manufacturer's catalogue for welding consumables.

Results for Hardness Testing

Hardness was measured on five specimens from every single welded plate. Table 4 shows received hardness values.

The received values are presented in Figure 6 in order to emphasize the observed effects of hardness increase.

Table 3 **Welding consumables data** [7]

WELDING CONSUMABLES	Chemical composition in mass / %		
	C	Si	Mn
FILTUB 12 B	0,05	0,35	1,40
Mechanical properties at standard room temperature			
$R_{p0,2}$ / N/mm^2	R_m / N/mm^2	A_5 / %	KV / J 20 °C, -20°C, -40°C
> 420	510-610	> 26	> 160, > 100, >60

Table 4 **HV 10 Hardness values for real weld samples – measured along the weld cross-section**

Sample mark	HARDNESS / HV 10											
	Measurements											
	1	2	3	4	5	6	7	8	9	10	11	12
R 101	188	186	218	262	345	274	275	339	292	231	186	187
R 102	183	185	215	253	322	270	268	330	262	238	187	190
R 103	190	191	218	287	344	282	285	335	292	230	186	188
R 104	181	185	218	262	342	282	284	337	272	231	182	183
R 105	187	185	218	262	347	278	273	341	292	237	183	185
R 111	188	186	221	240	306	254	260	317	262	236	193	188
R 112	189	186	225	248	286	262	260	290	252	232	186	187
R 113	188	186	229	256	297	258	259	293	252	228	190	187
R 114	187	185	219	224	273	255	252	269	248	223	186	189
R 115	188	186	217	237	274	262	260	275	241	213	184	185
R 121	185	181	201	227	279	224	225	287	243	208	181	188
R 122	187	189	217	237	267	234	235	264	235	215	191	193
R 123	188	186	229	235	263	232	234	268	237	214	193	195
R 124	188	186	210	239	269	230	228	267	241	203	183	185
R 124	190	187	216	237	271	227	229	273	234	213	186	187
R 131	185	182	193	220	240	209	210	246	215	198	181	180
R 132	183	186	191	218	241	205	207	244	222	194	187	190
R 133	190	191	205	232	246	213	215	240	225	207	186	188
R 134	191	187	194	215	245	219	221	248	212	195	185	183
R 135	187	185	190	216	250	209	214	250	221	197	188	189

Hardness values as measured along the cross-section and presented in Table 4 indicate that HAZ hardness decreases with extended cooling time $\Delta t_{8/5}$.

The maximal hardness values recorded in HAZ were around 345 HV for cooling time $\Delta t_{8/5}$= 5s; 317 HV for $\Delta t_{8/5}$ = 10s; 287 HV for $\Delta t_{8/5}$ = 25s and about 250 HV for $\Delta t_{8/5}$ = 50s.

Metallographic Examination of Particular Zones of the Real Weld Sample

After hardness determination, particular specimen zones were metallographically analyzed as given in Figures 7 to 10.

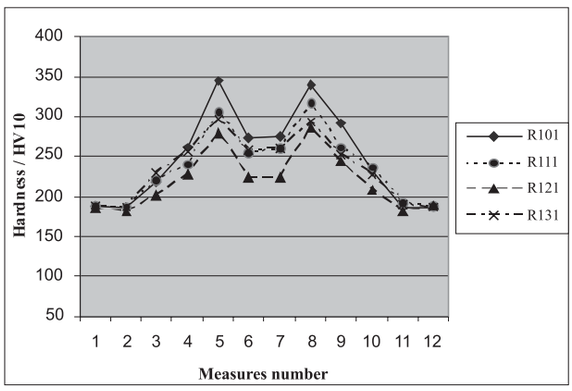

Figure 6. A comparison of hardness strains at different cooling times $\Delta t_{8/5}$: R101-$\Delta t_{8/5}$ = 5s; R111-$\Delta t_{8/5}$= 10s; R121-$\Delta t_{8/5}$ = 25s; R131-$\Delta t_{8/5}$ = 50s (data from Table 4, measurement according to Figure 1)

Result Data of the Impact Energy Analysis

The examination of the impact energy on real specimens was performed by using the Charpy method at temperatures of 20 °C, 0 °C, -20 °C and -40 °C. The results are presented in Figure 11.

Based on the diagram (Figure 11) the following can be concluded: For tested real weld samples, impact energy minima were obtained at cooling time $\Delta t_{8/5}$ = 5s. As cooling time $\Delta t_{8/5}$ increased, impact energy values also rose, but with a sequential drop between $\Delta t_{8/5}$= 25s and $\Delta t_{8/5}$ = 50s. As testing temperatures decreased, impact energy values dropped.

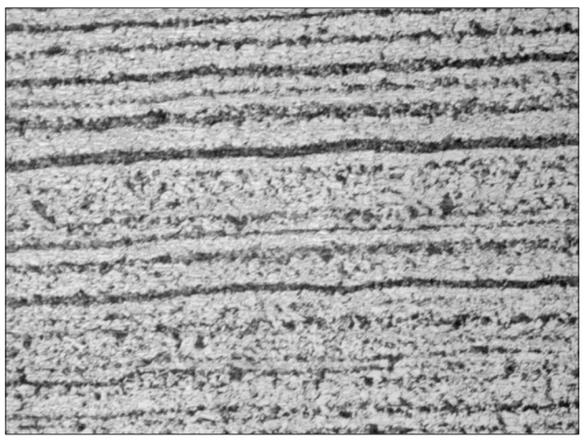

Figure 7. Microstructure of the base material TStE 420 normalized condition, magnification 200x

Results Obtained by Using the Electronic Microscope

The specimens were scanned on the electronic microscope, type "Quanta 200", manufactured by FEI (USA), at a magnification rate of 50 000 times. During testing, a vacuum of 5 x 10^{-3} Pa was achieved in the testing chamber. The experiment was conducted at the Faculty of Natural Sciences and Mathematics in Zagreb. Figures 11 and 12 show fracture surfaces of characteristic samples R111 and R311.

CONCLUSION

Micro-alloyed steels are weldable by using most of common technologies. Concerning hardness and tensile strength, weld properties generally match the base material properties. Cooling speed, i.e. cooling time $\Delta t_{8/5}$, greatly affects weld properties. By choosing optimal cooling speed, a satisfactory ratio between hardness and impact energy can be obtained, due to the formation of a microstructure less prone to the initiation and propagation of cold cracks. For purposes of experimental welding, on-line monitoring of welding parameter recording was used as a modern technology that allows better heat input determination and less ambiguous evaluation of welding stability. Testing of real weld specimens shows hardness decrease at HAZ at prolonged cooling time, as indicated in Figure 6. Maximal HAZ hardness was around 345 HV for cooling time $\Delta t_{8/5}$= 5s; 317 HV for

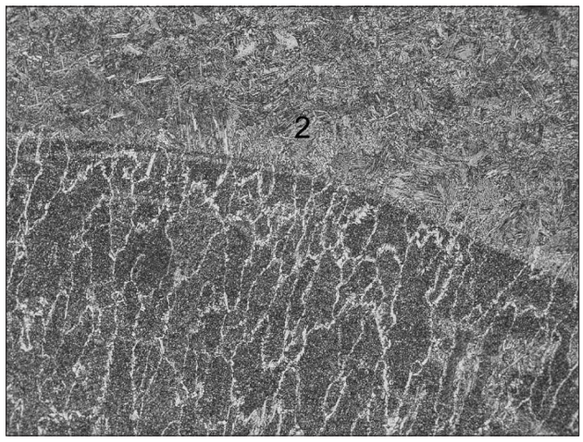

Figure 8. Microstructure of HAZ (2) in TStE 420 steel magnification 200x, $\Delta t_{8/5}$ =10s

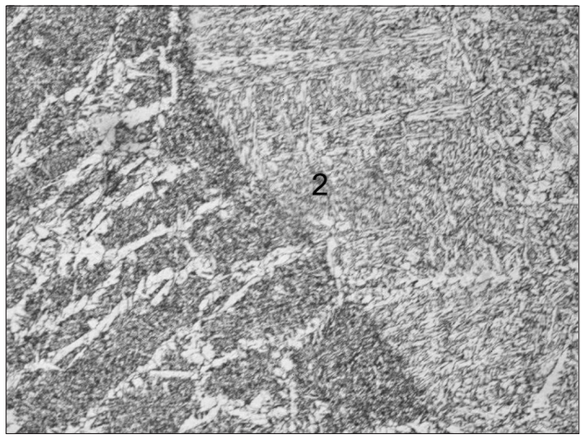

Figure 9. Microstructure of HAZ (2) in TStE 420 steel magnification 200x, $\Delta t_{8/5}$ =25s

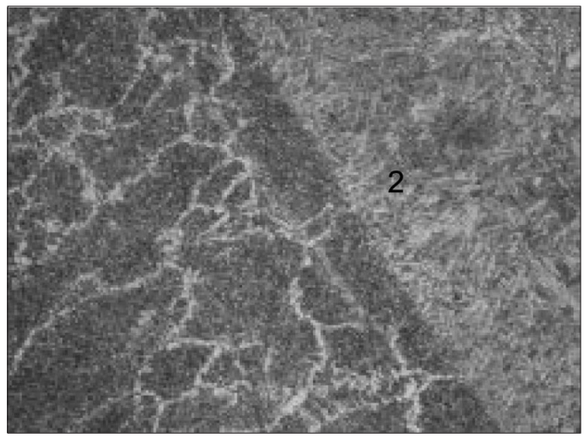

Figure 10. Microstructure of HAZ (2) in TStE 420 steel magnification 200x, $\Delta t_{8/5}$ =50s

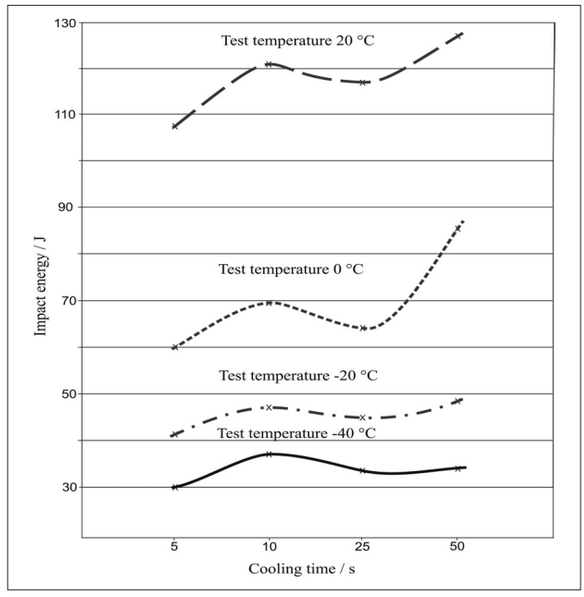

Figure 11. Relationship between impact energy and $\Delta t_{8/5}$ cooling time

Table 5 **Characteristics of real weld samples scanned on an electronic microscope**

SAMPLE MARK	R101	R301	R111	R311
KV / J	111,0	45,0	124,0	48,0
Testing temperature	20 °C	-20 °C	20 °C	-20 °C
Type of fracture	Ductile fracture	2/3 Ductile fracture	Ductile fracture	~ 80 Ductile fracture

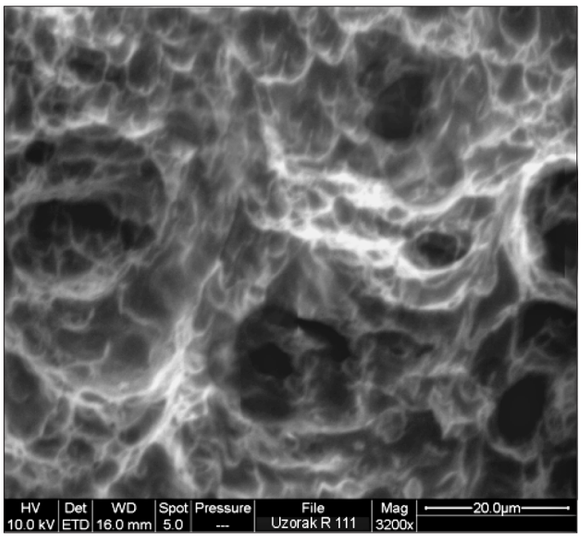

Figure 12. Fracture surface of the specimen R111

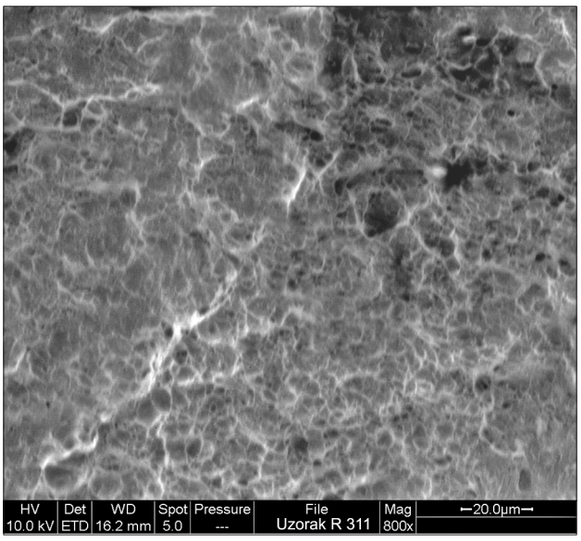

Figure 13. Fracture surface of the specimen R311

$\Delta t_{8/5}$ = 10s; 287 HV for $\Delta t_{8/5}$ = 25s and about 250 HV for $\Delta t_{8/5}$ = 50s. Impact energy of real weld specimens is the lowest at cooling time $\Delta t_{8/5}$= 5s. It increases at $\Delta t_{8/5}$ = 10s and drops thereafter - for $\Delta t_{8/5}$ = 25s it is slightly higher than at a cooling time of 5 s. As cooling time increases, impact energy also increases (Figure 11).

The microstructure of HAZ is rougher bainite-martensite (Figures 8 to 10). The weld microstructure is bainite-ferrite with pillar-type crystals.

The specimens were scanned on an electronic microscope in order to explain structural effects on impact energy. Typical examples of ductile and ~ 80% ductile fracture surfaces are shown in Figures 12 and 13. Structures as visible on the electronic scanning microscope suggest that the ratio of ductile fracture is above 30% for real weld samples.

Based on these experiments [8,9,10] and current practical experience, it is more favourable to perform welds in several passes if thicker HSLA is to be processed (in this test, base material thickness was δ = 15 mm). This is due to the fact that in a multi-pass method various specific microstructures within HAZ will appear along the melting line together with microstructures typical for one pass. Those microstructures positively affect mechanical properties when compared to one-pass real weld specimens.

REFERENCES

[1] Probst R., Herold H. Kompendium der Schweißtechnik, Schweißmetallurgie, DVS-Verlag GmbH, Düsseldorf, 1997.

[2] Winkler F. Schweißen von höherfesten Feinkornbaustählen. Böhler Schweißtechnik,Austria GmbH, 1989.

[3] Dunđer M., Samardžić I., Malina J. Weakening in arc welded joints due to temperature field nonstationary, Eurojoin 4, HDTZ, Cavtat-Dubrovnik, 2001.

[4] Samardžić, I., Dunđer, M. Contribution to weldability investigation of steel TSTE 420 on welding thermal cycle simulator. 8th international conference on production engineering (CIM), 2002., Brijuni (Croatia), pg. V65-v77, bibl. 3., UDK 621(063)658:52.011.56(063), ISSN 953-97181-4-7.

[5] Wegst C.W. Stahlschlüssel, Verlag Stahlschlüssel Wegst GmbH, Düsseldorf, 2001.

[6] MIZ DOC. IX-1609-90.

[7] Welding consumables, SŽ "Elektrode Jesenice", Jesenice 2004.

[8] Dunđer M. Doctoral thesis “Influence of cooling rate on hardness and toughness of micro alloyed steels“, FSB Zagreb, 2005.

[9] V. Gliha, Metalurgija, 44(2005)1, 13-18.

[10] J. Malina, I. Samardžić, V. Gliha. Materials Science, 41(2005)2, 253-258.

List of symbols

$\Delta t_{8/5}$ – Cooling time /s
$R_{p0,2}$ – Yield Strength /MPa
R_m – Tensile Strength /MPa
A_5 – Elongation /%
Z – Contraction /%
K_v – Impact energy /J
T_{max} – Maximal temperature /°C
T_0 – Room temperature /°C
I – Welding current /A
U – Voltage /V
v – Welding speed /cm/min
E - Heat input /J/mm

Note: Responsible translator: Željka Rosandić, professor of English and German language, Faculty of Mechanical Engineering University of Osijek, Slavonski Brod, Croatia.